

Mechanism of Synergistic Effects of Neutron- and Gamma-Ray-Radiated PNP Bipolar Transistors

Yu Song,^{1,2,*} Ying Zhang,^{1,2} Yang Liu,^{1,2} Jie Zhao,^{1,2} Dechao Meng,^{1,2}
Hang Zhou,^{1,2} Xiaofeng Wang,^{1,2} Mu Lan,^{1,2} and Su-Huai Wei^{3,†}

¹*Microsystem and Terahertz Research Center, China Academy of Engineering Physics, Chengdu 610200, P.R. China*

²*Institute of Electronic Engineering, China Academy of Engineering Physics, Mianyang 621999, P.R. China*

³*Beijing Computational Science Research Center, Beijing 100193, China*

(Dated: January 03, 2019)

The synergistic effects of neutron and gamma ray radiated PNP transistors are systematically investigated as functions of the neutron fluence, gamma ray dose, and dose rate. We find that the damages show a ‘tick’-like dependence on the gamma ray dose after the samples are radiated by neutrons. Two negative synergistic effects are derived, both of which have similar magnitudes as the ionization damage (ID) itself. The first one depends linearly on the gamma ray dose, whose slope depends quadratically on the initial displacement damage (DD) and can be attributed to the healing of neutron-radiation-induced defects in silicon. The second one has an exponential decay with the gamma ray dose, whose amplitude shows a rather strong enhanced low-dose-rate sensitivity (ELDRS) effect and can be attributed to the passivation of neutron-induced defects near the silica/silicon interface by the gamma-ray-generated protons in silica, which can penetrate the silica/silicon interface to passivate the neutron-induced defects in silicon. The simulated results based on the proposed model match the experimental data very well, but differ from previous model, which does not assume annihilation or passivation of the displacement defects. The unraveled defect annealing mechanism is important because it implies that displacement damages can be repaired by gamma ray radiation or proton diffusion, which can have important device applications in the space or other extreme environments.

I. INTRODUCTION

Radiating particles such as gamma ray and neutrons lead to ionizing (generating carriers) and non-ionizing (generating atomic displacements) energy depositions in semiconducting materials, respectively. As a result, the radiation damages of semiconductor devices contain both ionization damage (ID) and displacement damage (DD). In an environment with both gamma ray and neutron radiations, it is often assumed that the total damage is a simple sum of ID and DD. However, recent experiments have demonstrated that, the total damage in bipolar devices could be either smaller or bigger than the simple sum of ID and DD, that is, there is a negative or positive synergistic effect^{1–12}. However, the underlying mechanism of the synergistic effects is still not clear. It has been speculated that the gamma-ray-induced charged traps in silica near the silica/silicon interface can change the non-radiative Shockley-Read-Hall (SRH) carrier recombination by modifying charge distributions around the neutron-radiation-induced defects in the base region^{1,2}. For example, in PNP bipolar transistors, the accumulation of the positive oxide trapped charge (N_{ot}) near the interface increases the electron density near the base surface by Coulomb attraction (see Fig. 1a). As a result, the SRH recombination current is suppressed because of the widened carrier density difference in the base region, i.e., a negative synergistic effect arises. In NPN devices, a positive synergistic effect would arise because the positive oxide trapped charge lowers the hole density near the base surface through Coulomb repulsion, which reduces the difference of carrier densities in the base region, thus

enhances the SRH recombination current. It has also been speculated that the gamma-ray-induced interface traps on the silica/silicon interface can also modify the charge distribution and change the SRH recombination. However, since the interface traps are negative (positive) in N-type (P-type) base region, they always induce a positive synergistic effect for both PNP and NPN transistors^{5–7}. Very recently, it is deduced from deep level transient spectroscopy (DLTS) signals that the positive synergistic effect in NPN transistors can be enhanced by the displacement defects generated in the oxide layer by low-energy proton radiations, because the defects can induce more oxide trapped charge during sequential high-energy proton radiations^{11,12}. All these models assume that in these processes, the neutron-radiation-induced defect density in the base region is not affected by the gamma ray radiation. However, no systematic study has been carried out to confirm the assumption and moreover, it is not clear what is the dependence of the synergistic effects as functions of the neutron fluence, gamma ray dose, and dose rate.

In this work, we carry out systematic investigation on the mechanism of the negative synergistic effects observed in PNP bipolar transistors. The input-stage PNP transistors in the widely used operational amplifiers LM324N are successively radiated by neutron and gamma ray with different neutron fluence, gamma ray dose, and dose rates. We observe a ‘tick’-like dependence on the gamma ray dose on samples radiated by neutrons, from which we identified two negative synergistic effects that have magnitudes comparable with the ID itself. The first one depends linearly on the gamma ray dose, whose

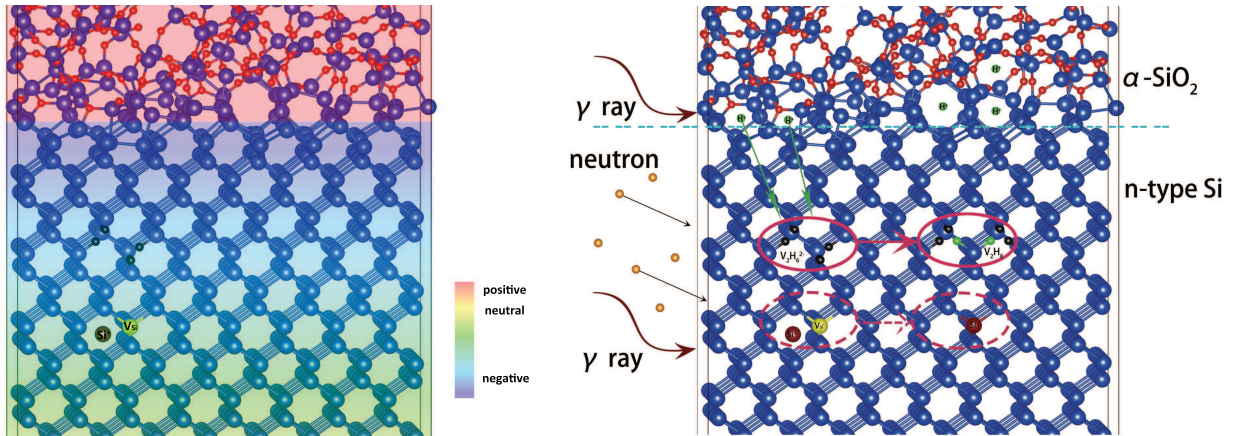


FIG. 1. (color online) Schematic diagram for the mechanisms of negative synergistic effect in PNP transistors. (a) One of the traditional models^{1,2} in the literature: the Coulomb interaction of gamma-ray-induced trapping charge in silica (red background) on the majority charge carriers (electrons) in silicon (green and blue background), which leads to a change in the concentration of charge carriers and SRH recombination rate in silicon. (b) The unraveled mechanism in this work: the gamma-ray radiation can heal the neutron-radiation-induced defects (vacancies and interstitials, dashed circle) and the induced protons in silica can also penetrate the interface to passivate the defects in silicon near the silica/silicon interface (V_2H_6 etc., solid circle), which lead to a decrease of the concentration of the SRH recombination centers in silicon.

slope depends quadratically on the initial DD. The second one has an exponential decay with the gamma ray dose, whose amplitude shows a rather strong enhanced low-dose-rate sensitivity (ELDRS) effect. To explain the observed data, we propose a *defect annealing* model containing two terms, a carrier-induced defect annihilation in silicon and a proton-induced defect passivation near the silica-silicon interface, which are schematically shown in Fig. 1(b). The simulated results based on the proposed model match the experimental data very well, but differ from previous model that does not consider defect annihilation or passivation. Our unraveled mechanism is important because it implies that, we can repair damaged silicon devices used in space or under other extreme environments by applying appropriate gamma radiation or proton diffusion.

The paper is organized as following. In Sec. II, we describe the experimental setup of the neutron-gamma radiations. In the following Sec. III A, we first show the data, which are found to display clear ‘tick’-like damage-dose profiles. We then demonstrate the presence of two negative synergistic effects in Sec. III B. We then analyze the origin of the two negative synergistic effects in Sec. III C and Sec. III D, respectively. The relative strength of the two negative synergistic effects and experimental conditions for the ‘tick’-like profiles are investigated in the Sec. III E and Sec. III F, respectively. The conclusion is made in Sec. IV.

II. EXPERIMENTAL SETUP

To investigate the behavior of the negative synergistic effect in PNP transistors, LM324N chip (Texas Instru-

ments, TI) with 4 operational amplifiers in each chip was selected for this study. This is because the input stage of the operational amplifier is very straightforward hence the input bias current is directly related to the base current of the input-stage PNP transistors^{13,14}. Based on this fact, the synergistic effect of the input bias current of an LM124 chip, which is very similar to LM324N, has been understood and modeled in the level of the input-stage transistors^{1,2}. On the other hand, with a substrate structure and lightly doping, the input-stage transistors in LM324N are sensitive to both neutron and gamma ray radiations,^{1,2} which is essential for observing a remarkable synergistic effect. The processes of the experiments are shown in Fig. 2. Six neutron-gamma conditions are employed: first neutron radiation with the fluence of $2 \times 10^{13}/\text{cm}^2$, $3 \times 10^{13}/\text{cm}^2$, and $5 \times 10^{13}/\text{cm}^2$,

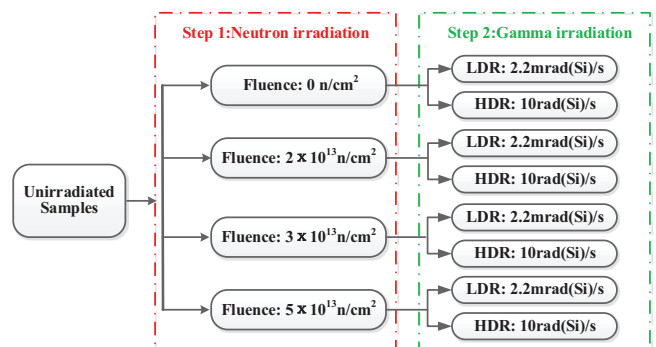


FIG. 2. (color online) Flowchart of the neutron/gamma radiation experiments. For each of the eight radiation conditions, 2 chips with 8 PNP transistors are used.

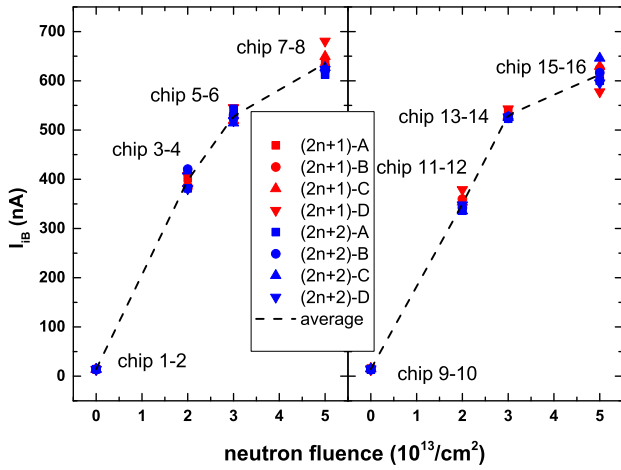


FIG. 3. (color online) The input bias current of the input-stage PNP transistors in LM324N as a function of the neutron fluence. The measurements are performed 15 days after the neutron radiations are over. The temperature during radiation, storage, and measurements are 20°C . For each fluence ($n=0-7$), the two chips are distinguished by different colors of red and blue, respectively; in each chip, the four transistors (labeled as A, B, C, and D) are distinguished by different symbol shapes of square, circle, up-triangle, and down-triangle, respectively.

respectively; then gamma radiation to 5krad(Si) at a low dose rate of 2.2 mrad(Si)/s and a high dose rate of 10 rad(Si)/s, respectively. Another two pure gamma radiation conditions are used to obtain the artificial damage. For each condition, we use 2 chips (i.e., 8 PNP transistors). In all the experiments, chips were radiated in an unbiased configuration with all pins shorted. The input bias currents were measured by BC3193 discrete semiconductor testing systems and used to analyze the damages of the input-stage PNP transistors. Neutron radiations were performed at the Chinese Fast Burst Reactor-II (CFBR-II) of Institute of Nuclear Physics and Chemistry, China Academy of Engineering Physics, which provides a controlled 1MeV equivalent neutron radiation. Gamma ray radiations were done at College of Chemistry and Molecular Engineering of Peking University.

III. RESULTS AND DISCUSSION

A. ‘Tick’-like dependence on the gamma ray dose

The samples are first radiated by neutrons. Fig. 3 shows the pure DD response of the studied devices. The transistor numbers are indicated in the figure. Also plotted is the average value of the 8 PNP transistors for each neutron fluence. It is seen that, the input bias current (I_{iB}) increases sub-linearly with the neutron fluence. When the neutron fluence accumulates from 0 to $5 \times 10^{13}/\text{cm}^2$, the average bias current increases from about 10 nA to about 600 nA. Due to the different

sample quality, the DD of 8 transistors under a same fluence are also different by tens of nA, which will lead to different latter gamma ray response, as discussed below. The thin oxide layer in the PNP transistor is almost transparent for neutrons¹⁵. Neutron radiation has been shown to introduce acceptor-like defects in Si¹⁶⁻¹⁹. The divacancies (V_2) and vacancy-oxygen (VO) pairs prominently identified in DLTS measurements^{20,21} are thought to be the candidates for these negative charged defect centers^{19,20,22}, see Fig. 1(b). Accompanying, Si self-interstitials are also generated. The lifetime of minority carrier (τ) is inversely proportional to the concentration of defects.²³ Accordingly, the generation of defects with an increase of neutron fluence results in a persistent decrease of the lifetime of minority carrier and hence the DD degradation,²⁴

$$\Delta I_{iB}^D = \frac{qn_i A x_{dB}}{2\tau} e^{\frac{qV_{BE}}{2k_B T}}. \quad (1)$$

Here the superscript D stands for DD, q is the charge of minority carrier, n_i is the concentration of intrinsic carriers, A and x_{dB} are the area and depth of the space charge region, respectively, V_{BE} is the bias between the base and emitter electrodes, and T is the temperature. This relation implies that the concentration of the generated defects is proportional to the increase of the input bias current, $[V] = \lambda \Delta I_{iB}^D$, where $\lambda^{-1} \propto \frac{qn_i A x_{dB}}{2} e^{\frac{qV_{BE}}{2k_B T}}$. From the data as shown in Fig. 3, we can see that the concentrations of the generated defects in silicon are different for different neutron fluence and samples.

To obtain the simple sum of DD and ID, chips No. 1-2 and No. 9-10 are radiated by gamma ray with low and high dose rate, respectively. The results are displayed in Fig. 4(a) and 4(e), respectively. It is seen that, the ID increases almost linearly with the gamma ray dose, i.e., $\Delta I_B^I = k_0 x$, where x is the gamma ray dose in unit of krad(Si). An average coefficient of $k_0^L = 16.0$ nA/krad(Si) and $k_0^H = 7.0$ nA/krad(Si) are obtained for the low and high dose rate, respectively. There is a clear ELDRS effect²⁵, with an enhancement factor of about 2.3. Under gamma ray radiations, protons are generated in the silica layer through dissociation reactions between oxide trapping charges and hydrogen molecule^{26,27}, see Fig. 1 (b). The generated protons diffuse to the oxide/silicon interface and further generate interface traps (N_{it}) through depassivation reactions on passivated defects Si-H bonds on the interface^{26,28}. The interface traps result in an increase in the surface recombination velocity (Δs) above the base region, which leads to the base current increment^{29,30}

$$\Delta I_{iB}^I = \Delta s \frac{qn_i P_E x_{dB}}{2} e^{\frac{qV_{BE}}{2k_B T}}. \quad (2)$$

Here the superscript I stands for ID, $\Delta s = v_{th} \sigma \Delta N_{it}$, where v_{th} is carrier thermal velocity and σ is the carrier capture cross section. P_E is the emitter perimeter. From the data in Fig. 4 (a) and (e), it is seen that N_{it} increases linearly with the gamma ray dose. The concentration of

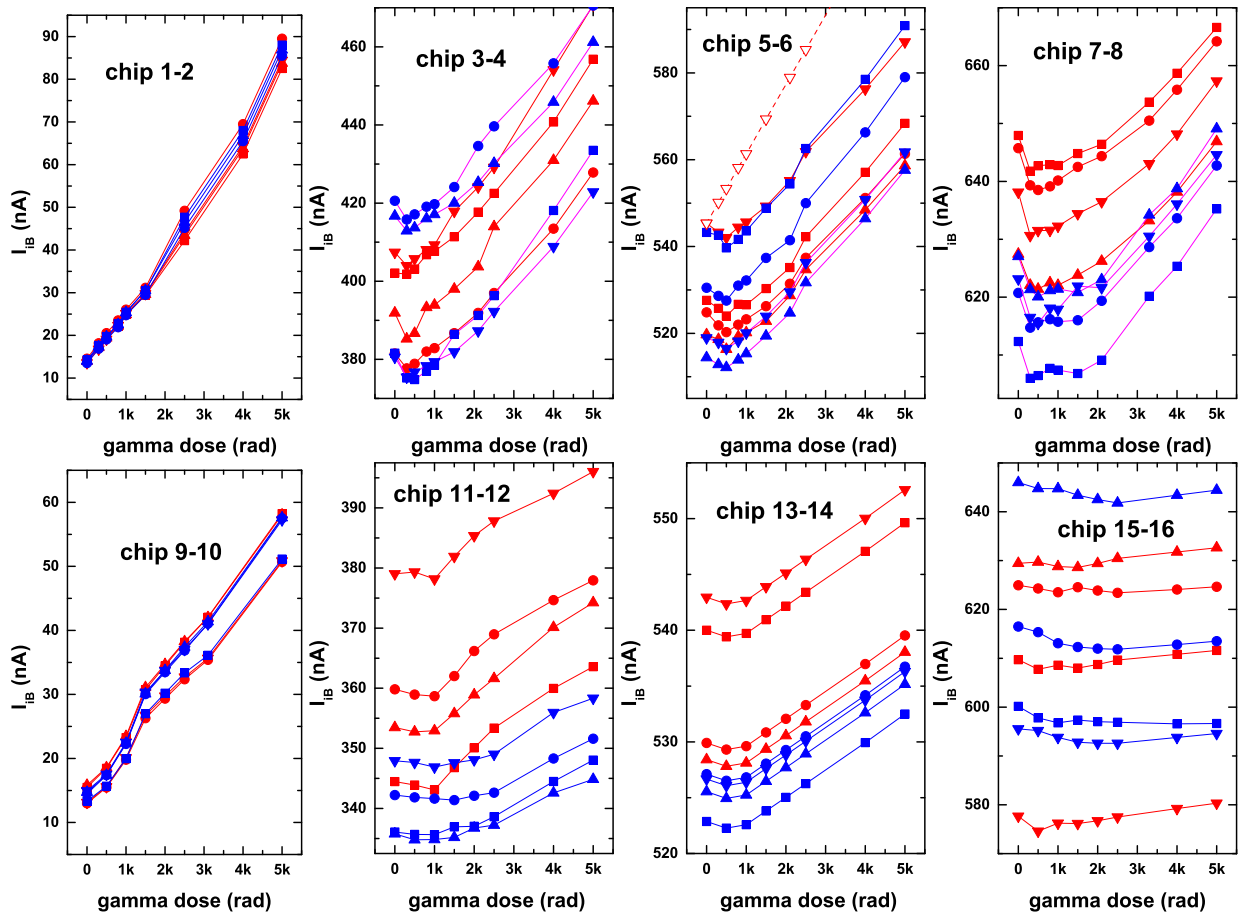


FIG. 4. (color online) (a)-(d) The input bias current as a function of the gamma ray dose at low dose rate of 2.2 mrad(Si)/s for PNP transistors under radiations of different initial neutron fluence. From left to right, the neutron fluence is 0, $2 \times 10^{13} \text{ cm}^{-2}$, $3 \times 10^{13} \text{ cm}^{-2}$, and $5 \times 10^{13} \text{ cm}^{-2}$, respectively. (e)-(h) The same configurations as (a)-(d) but at a high dose rate of 10 rad(Si)/s. In each split, the two chips are distinguished by different colors of red and blue, respectively; in each chip, the four transistors are distinguished by different symbol shapes of square, circle, up-triangle, and down-triangle, respectively.

the generated protons is almost constant, which is higher for the low dose rate case.

The simple sum of the DD and ID damages then reads:

$$\Delta I_{iB}^{D+I} = D_0 + k_0^{L(H)} x, \quad (3)$$

where D_0 is the initial DD. The result is plotted in Fig. 4(c) for transistor No. 5D. The low-dose-rate gamma response of chips No. 3-8 (24 transistors) with various D_0 are shown in Fig. 4 (b-d). Similarly, the high-dose-rate gamma response of chip No. 11-16 (another 24 transistors) are shown in Fig. 4 (f-h). It is seen that, for all 48 samples the total damages are smaller than the simply summed ones. In other words, a clear negative synergistic effect is observed. In previous works^{1,2}, this effect is attributed to the change of the electron density in silicon caused by positive oxide charge accumulation in silica, see Fig. 1(a). However, in this work, our analysis of the features in the data suggest that these effects are due to the annihilation and passivation of the DD defects in silicon.

The damages display a ‘tick’-like profile: they abnormally decreases for small gamma ray dose and then increase almost linearly for large gamma ray dose. However, the slope for the latter is obviously smaller than k_0^L or k_0^H . In the following, we will show that, they result from the *proton passivation and carrier-induced annihilation of the neutron-radiation-induced defects* in silicon, respectively.

B. Linear and exponential negative synergistic effects and their fluence and dose rate dependence

To obtain a general trend as a function of the initial displacement damage and gamma ray dose rate, in Fig. 5, we plot six typical damage-dose curves: three with D_0 of about 380nA, 520nA, and 610nA radiated with the low dose rate, and three with D_0 of about 350nA, 520nA, and 630nA radiated with the high dose rate. It is seen that, the larger the initial DD, the bigger the decrease in the slope at large gamma ray dose; on the other hand, the

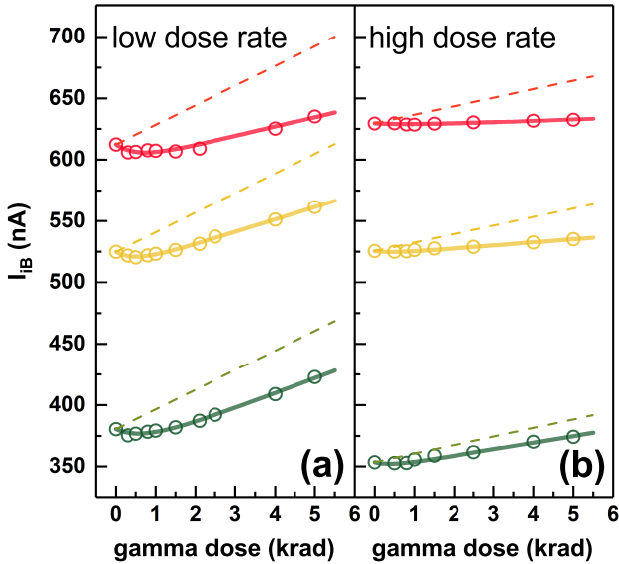


FIG. 5. (color online) The experimental data (dots) and fitting curves (solid) of the input bias current as function of gamma ray dose of samples with various initial DD. (a) The case of transistors radiated with low dose rate. (b) The case of transistors radiated with high dose rate. The simple combined damages are plotted by the dashed lines.

lower the dose rate, the stronger the abnormal decrease of the damage at small gamma ray dose.

To further investigate the possible origin of these two synergistic effects, we fit all the data for the low/high dose rate case in Fig. 4(b-d)/(f-h). Considering both the linear behavior at the large gamma ray dose and the exponential-like decline at the small gamma ray dose in the damage-dose curves, we find that the negative synergistic effects of all 48 curves with different nonzero D_0 in Fig. 4 can fit very well to the relatively simple function containing a negative linear term and a negative exponential term,

$$\Delta I_{iB} = \Delta I_{iB}^{D+I} - ax - b(1 - e^{-cx}). \quad (4)$$

Here a is the deviation slope of the linear term; it has a dimension of nA/krad. b has a dimension of nA and stands for the amplitude of the exponential decay term. c describes the decay rate; its dimension is 1/krad. The fitted curves for the six typical samples are shown in Fig. 5. The individual linear synergistic term $-ax$ and the exponential synergistic term $-b(1 - e^{-cx})$ for the 3 curves with different D_0 in Fig. 5(a) are shown in Fig. 6 for further analysis. It is clear that, there are two separate negative synergistic effects in the investigated system.

The fitting decay rate (c) is found to be insensitive to the neutron fluence or gamma ray dose rate. It is almost the same ($c = 2.1/\text{krad}$) for all 48 damage-dose curves. The fitting parameters a and b as a function of D_0 for samples radiated at the low/high dose rate are shown in Fig. 7 (a) and (b), respectively. It is seen that, the decrease in the slope of the damage (a) increases with

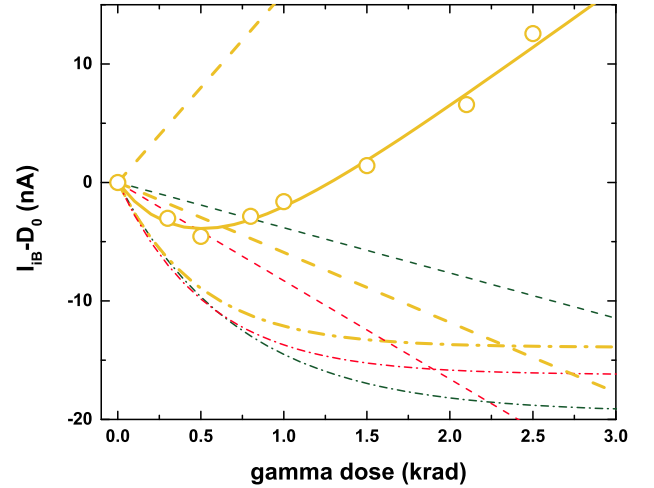


FIG. 6. (color online) The decomposition of the damage-dose curve with medium DD (orange) in Fig. 5(a). Dashed line is for the linear annealing effect and dash-dot curve is for the exponential annealing effect. For comparison, the linear and exponential terms for damage curves with low and high DD (green and red, respectively) in Fig. 5(a) are also plotted. For clearness, the initial DD is deducted from the input bias currents.

D_0 superlinearly. Further fitting of the a - D_0 data shows that, an interesting and simple relation is satisfied for both the low and high dose rates,

$$a = \alpha D_0^2, \quad (5)$$

where $\alpha = 21/(\text{mA} \times \text{krad})$ and $\alpha = 16/(\text{mA} \times \text{krad})$ for the low and high dose rate case, respectively. On the other hand, the amplitude of the exponential term (b) shows a strong dose rate dependence and is not very sensitive to the initial displacement damage.

C. Dependence of the linear synergistic effect on the neutron fluence: carrier-induced defect annihilation in silicon

We first consider the origin of the linear synergistic effect. According to Eqs. (4) and (5), the linear synergistic term can be re-written as

$$\Delta I_{iB}^{SE1} = -\alpha D_0^2 x. \quad (6)$$

This expression suggest the following. 1) The term depends exactly on D_0 , which means that this synergistic effect is related to the neutron-induced defects in silicon; 2) The term is negative, which means that the neutron-induced defects is reduced. In other words, *an annealing effect of the neutron-induced defects in silicon* happens. 3) The term is a quadratic function of the defect concentration, which suggest that the annihilation of two kinds of related defects happens; 4) The term also depends linearly on the gamma ray dose, which means that the

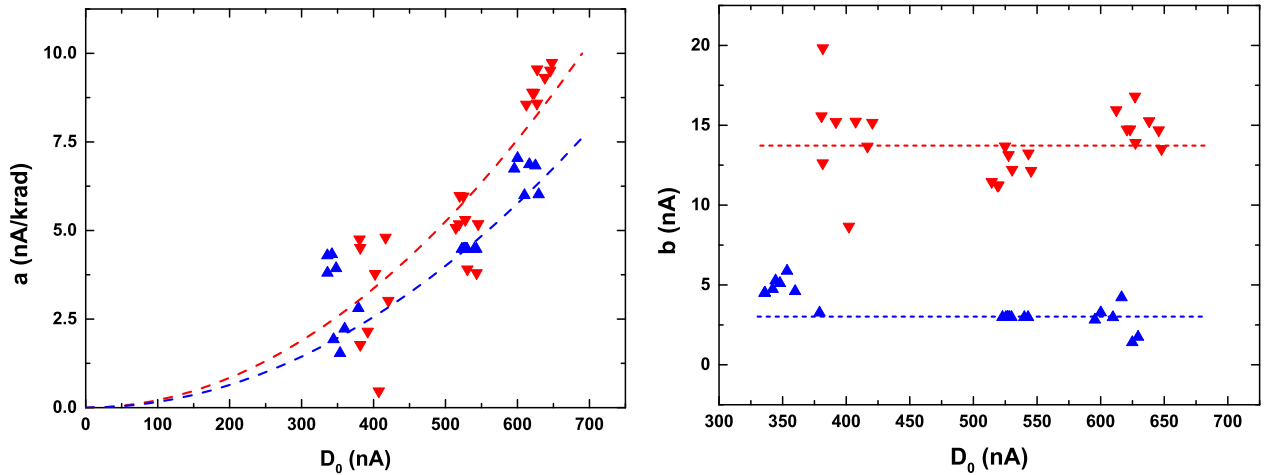
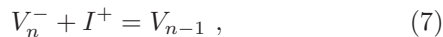


FIG. 7. (color online) (a, b) The fitting parameters a and b in Eq. (4) for the 48 curves in Fig. 4 as a function of the initial displacement damage. The fitting value of c is 2.1/krad for all samples. Red for the low dose rate and blue for the high dose rate.

annihilation of the neutron-induced defects is induced by gamma-induced charge carriers.

This observation clearly cannot be attributed to the charge redistribution in the silicon region as implied in early models.^{1,2,5-7} Here, we propose that the defect annihilation can be described by the following annihilation reaction



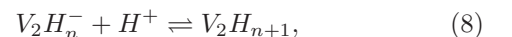
where V is the vacancy and I is the Si interstitial, both of which are charged by the gamma radiation, see Fig. 1(b). We note that the annihilation of defects in silicon due to injected charge carriers has been found in the past³¹⁻³³ and the origin has been attributed to the enhanced mobility of defects through alternating capture and loss of electrons.³⁴⁻³⁸ Among various defects, the isolated Si interstitial defects are mobile particles. From this reaction, we can see that, for a fixed gamma ray dose rate, the more the neutron-induced defects exist in the sample the easier to find I^+ as well as V_n^- . On the other hand, for a fixed defect concentration, the more the charge carriers ($[h]$) are excited by the γ -ray, the more the mobile defects are stimulated. According to the chemical reaction rate equation, the annihilation rate of the vacancies reads $d[V_n^-]/dt = -k_a[V][I][h]$, where k_a is the reaction rate constant between the excited vacancies and interstitials. A simple calculation gives $\Delta V_n^- = -k_a[V][I]x$, where $x = [h]t$ is the gamma ray dose. Here the defect concentrations on the right side in the reaction rate equation are much larger than the change and are regarded as constants during the gamma ray radiation. Recalling the relation between the defect concentration and DD, $[V] = [I] = \lambda D_0$, the above relation can be rewritten as $\Delta I_{iB}^{SE1} = -k_a \lambda D_0^2 x$. This is just Eq. (6), with $k_a \lambda$ corresponding to α . As mentioned above, the value is a slightly larger for the low dose rate case (21/(mA \times krad)) than for the high dose rate (16/(mA \times krad)), with an en-

hancement factor of about 1.3. This means that there is also an ELDRS effect in the linear synergistic effect. It can be concluded that, the square law come from the fact that, the annihilation requires the existence of both interstitial and vacancy; while the interstitial defect caused by the neutral radiation has the same quantity as the vacancy defect.

D. Dependence of the exponential synergistic effect on the gamma ray dose rate: proton-induced defect passivation near the silica-silicon interface

Having understood the origin of the linear synergistic effect, we now investigate what is the origin of the exponential synergistic effect, $-b(1 - e^{-cx})$ in Eq. (4). As we can see in Fig. 7 (b), the amplitude of the exponential synergistic term (b) shows an evident ELDRS effect. For the lower dose rate, b has a higher value of about 13.5nA, while for the higher dose rate, b has a smaller value of about 3.0nA. Accordingly, the enhancement factor is 4.5, which is about two times of that for the pure ID, see Figs. 4 (a) and (e). As mentioned before, protons play a central role in the ELDRS effect of the ID.²⁵ Thus, the strong ELDRS effect of the exponential synergistic effect suggests proton is involved in the process. To test this assumption, we did further analysis in the following.

Some experiments and theories have shown that, hydrogen can penetrate the a-SiO₂/Si interface³⁹ and diffuse into Si⁴⁰⁻⁴². Further, other experiments and theories also show that, hydrogen is capable of passivating various types of acceptor-like defects and extended defects in Si^{40,41,43-52}. Many types of complex have been proposed, including V_2H_6 , V_2H_8 , VH_2 , VH , etc^{43,46,53}. The representative reactions can be described as



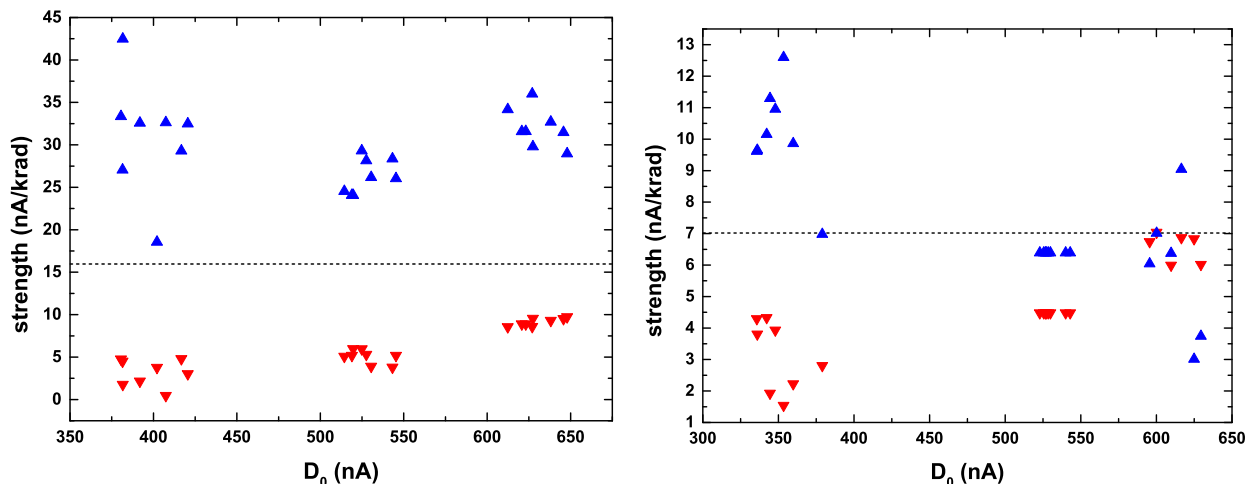


FIG. 8. (color online) (Initial) strength of the charge- and proton-induced synergistic effects (red and blue) as a function of the initial DD for the (a) low and (b) high dose rate. The strengths for the ID are shown as the dashed lines.

where V_2H_{n+1} is electrically non-active, see Fig. 1(b). These reactions remove the band-gap levels in silicon thus reduce the recombination rate (decrease the displacement damage).

Supposing the concentration of V_2H_n contributes a base current of D_1 . From Figs. 5 and 7(b), it is clear that, D_1 (about several nA) is much less than D_0 (about hundreds of nA). This means that, the concentration of V_2H_n is much fewer than the total amount of the neutron-induced defects in silicon. Thus, not many protons are required to totally anneal the former defects. The relation also means that, the reaction of Eq. (8) can cause sensible changes to the concentration of V_2H_n . In other words, the concentration is an explicit function of time, $V_1(t)$. From Eq. (8), the decay rate of $V_1(t)$ is $d[V_1](t)/dt = -k_p[H][V_1](t)$, where k_p measures the reaction rate between the defects and protons. Integrating the equation, the defect concentration as a function of time (gamma ray dose) is obtained as

$$V_1(t) = V_1 e^{-\beta x}, \quad (9)$$

where we have replaced $k_p[H]t$ with βx . Accordingly, the input bias current changes from D_1 to $D_1 e^{-\beta x}$, which results in a current decrease of

$$\Delta I_{iB}^{SE2} = -D_1(1 - e^{-\beta x}). \quad (10)$$

Eq. (10) has the same form as the exponential term in Eq. (4), with the amplitude D_1 corresponding to the fitting factor b and the effective decay rate β corresponding to the fitting factor c .

The reasons for the strong ELDRS effect of the amplitude of the exponential synergistic effect can be explained as following. 1) For the lower dose rate, more protons are generated in silica as a result of the ELDRS effect of the ID, so more protons can diffuse into silicon and leads to a larger passivation. 2) For the lower dose rate, there

is a much longer time for protons to diffuse into silicon, which further increases the difference of the amount of the protons in silicon. So, it can be concluded that, the exponential synergistic effect stems from the defect passivation near the silica-silicon interface, which is induced by protons diffusing from the silica, see Fig. 1(b).

The variable β or c shows no evident dependence on D_0 or the gamma ray dose rate. This is because it measures an intrinsic interaction strength, whose value does not depend on the concentrations of the reactants ($V_2H_n^-$ and H^+), which are determined by D_0 or the dose rate.

E. The relative strength of the two synergistic effects

By combining Eqs. (2), (6), and (10), the practical neutron-gamma damage is described by the following equation:

$$\Delta I_{iB}^{syn} = D_0 + k_0 x - \alpha D_0^2 x - D_1(1 - e^{-\beta x}). \quad (11)$$

It is clear that, the practical damage deviates from the simple summed one ($D_0 + k_0 x$) by two synergistic effects, namely the carrier-induced linear annihilation, $-\alpha D_0^2 x$, and the proton-induced exponential passivation, $-D_1(1 - e^{-\beta x})$. This is very different from the existing mechanism: Coulomb interaction induced change in the concentration of charge carriers in silicon. Now an important question would arise: How strong are the two synergistic effects? Should they be weak enough that they can be neglected? To answer this question, we derive the changing rates of the input bias currents by taking derivative of ΔI_{iB}^{syn} in Eq. (11) with respect to x . The result is

$$\frac{d\Delta I_{iB}^{syn}}{dx} = k_0 - \alpha D_0^2 - \beta D_1 e^{-\beta x}. \quad (12)$$

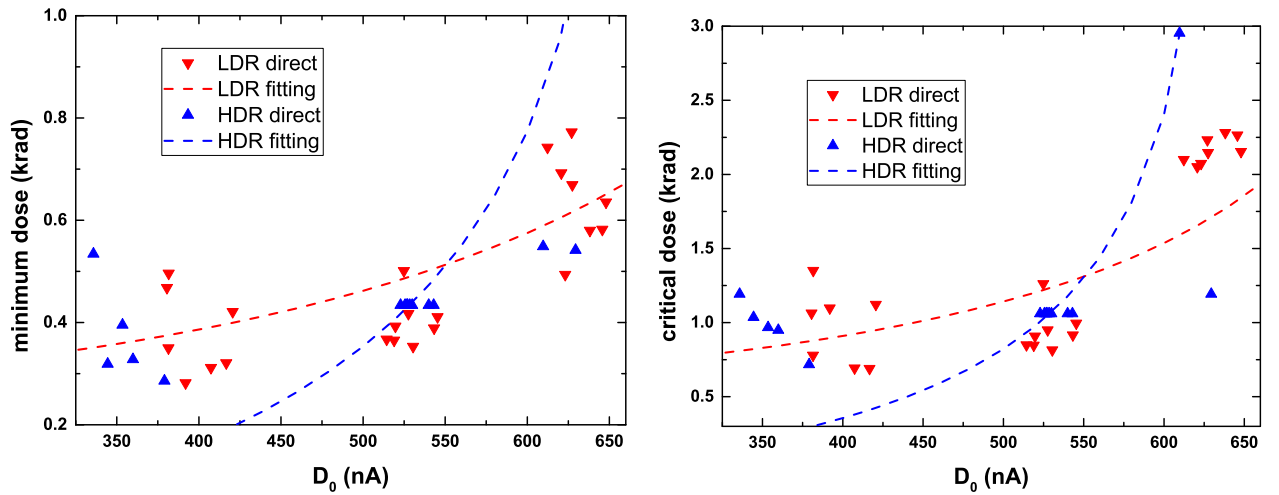


FIG. 9. (color online) The (a) minimal and (b) critical damage dose as a function of the initial DD. Dots are for values directly read from the data and curves are for results calculated by Eq. (14) or (16). Red is for the low dose rate and blue is for the high dose rate.

Thus, the strength for each effect can be defined as the corresponding slope, which reads k_0 , αD_0^2 , and $\beta D_1 e^{-\beta x}$ for the ID, the carrier-induced linear annihilation, and the proton-induced exponential passivation, respectively. It is seen that, the strength for the proton-induced passivation decays with the time. In the following, we would like to discuss the initial strength βD_1 . The values of αD_0^2 and βD_1 are plotted in Fig. 8 (a) and (b) for the low and high dose rate, respectively. The values of k_0^L and k_0^H are indicated by the dashed lines. For the low dose rate case, it is seen that, the strength of the carrier-induced annihilation, which increases with the initial DD, is a little smaller than the strength of the ID, while the initial strength of proton-induced passivation is stronger than the strength of the ID. The cases for the three typical samples radiated with the low dose rate can be clearly seen in Fig. 6. For the high dose rate case, both the carrier-induced annihilation and the proton-induced passivation are comparable with the ID. So, although the two negative synergistic effects (of the order of nA) are much smaller than the initial DD (of the order of hundreds of nA), they are comparable with the ID.

It is interesting that, the initial strength of the proton-induced passivation (βD_1) is larger than the strength of the carrier-induced annihilation (αD_0^2), although the population of the defects involved in the former ($\propto D_1$) is about two order of magnitudes smaller than the population of the defects involved in the latter ($\propto D_0$). The reason is that, the reactions in the proton-induced passivation are much easier than the reactions in the carrier-induced annihilation, because the $V_2H_n^-$ defects in the former contain dangling bonds and the binding energy with protons are negative^{43,46,53}.

F. Conditions for the ‘tick’-like profiles and specific damages

The ‘tick’-like damage-dose profiles in Figs. 4 and 5 are essential to obtain the two negative synergistic effects. In this last subsection, we will try to investigate under which neutron fluence such a profile can arise. To further verify the proposed model (Eq. (11)), we will also calculate under what gamma ray dose the damage will become the minimal or the same as the initial one, and compare the results with the experiment data.

From Eq. (12), it is readily seen that, if the sum of the (initial) strengths of the two synergistic effects are larger than the strength of the ID, the positive ID term will be overwhelmed and the damage-dose curves will show the declining behaviors. For large enough gamma ray dose, the strength of the proton-induced passivation almost vanishes and the damage-dose curves show ascending behaviors, provided the strength of the ID is stronger than that of the linear annealing. So, the conditions to display a ‘tick’-like profile is that, the ID is smaller than the sum of two annealing effects but larger than the linear annihilation effect. In the view of initial DD (neutron fluence), this means that the carrier-induced annealing should be stronger than the difference between the ID and the proton-induced passivation, but smaller than the ID itself,

$$\sqrt{\alpha^{-1}(k_0 - \beta D_1)} < D_0 < \sqrt{\alpha^{-1}k_0}. \quad (13)$$

For the low dose rate, we obtain $D_0 < 872.9$ nA for the appearance of the ascending behavior at large gamma ray dose and no requirement for the declining behaviors at the small dose. For the high dose rate, we obtain 237.2 nA $< D_0 < 661.4$ nA for the appearance of the ‘tick’-like profiles. These conditions are consistent with the experimental data in Fig. 4. On the other hand, we have

obtained monotonously decreasing damage-dose profiles with high gamma ray dose rate for D_0 of about 1000 nA (using neutron fluence of $1 \times 10^{14}/\text{cm}^2$).

At a gamma ray dose where the derivative of the input bias current on the gamma ray dose becomes zero, the damage reaches its minimal value. From Eq. (12), the gamma ray dose is obtained as

$$\beta x_{min} = \ln\left(\frac{\kappa}{k}\right), \quad (14)$$

where $k = k_0 - \alpha D_0^2$ and $\kappa = \beta D_1$. Physically, this equation means that, at the specific dose of x_{min} the decrease rate of the base current due to the two kinds of defect annealing in silicon equals to the increase rate of the base current due to the defect generation on the interface. Inserting this condition into Eq. (11), the minimal current is obtained as

$$I_{iB}^{min} = D_0 + D_1 \left[\frac{k}{\kappa} \ln\left(\frac{\kappa}{k}\right) - \left(1 - \frac{k}{\kappa}\right) \right]. \quad (15)$$

The calculated curve using Eq. (14) is shown in Fig. 9 (a) for both the high and low dose rates. Also shown are the dose values for each sample, which is directly read from the data in Fig. 4. For the low dose rate case, the calculated curve is found to have good agreements with the experimental data, further implying the validity of the proposed model. However, for the high dose rate case, the agreement is only good for the curves with initial DD of about 530nA in Fig. 4 (g). This is because the dose step of 0.5krad (total dose of 5krad) is too large (small) for the curves with D_0 of about 350nA (610nA) in Fig. 4f (4h) and the true dose values can be easily missed. From the model predictions, it is also seen that, for both the high and low dose rates, the dose condition for the minimal damage increases for the increasing D_0 .

For certain larger gamma ray dose, the damage returns to the initial value before gamma radiation (i.e., D_0), which we can call as a critical dose. Solving Eq. (11) with the condition of $\Delta I_{iB}^{syn} = D_0$, the critical gamma ray dose is obtained as

$$\beta x_c = \frac{\kappa}{k} + W\left[-\frac{\kappa}{k} e^{-\frac{\kappa}{k}}\right], \quad (16)$$

where W is Lambert-W function or product logarithm. Physically, this equation means that, at the specific dose of x_c the base current due to the two kinds of defect annealing in silicon equals to the base current due to

the defect generation on the interface. Again the calculated curve using Eq. (16) and the experimental data are shown in Fig. 9 (b), which are found to be in good agreement with each other for the low dose rate case. For the high dose rate case, the agreement is bad for the samples with D_0 of about 350nA (610nA), due to the too large dose step (too small total dose). It can be seen that, for both the high and low dose rates, the critical dose depends monotonously on the initial DD.

It has been noticed that, the ratio of the strength of the proton-induced passivation ($\kappa = \beta D_1$) and the sum of the strengths of the ID and the charge-induced annihilation ($k = k_0 - \alpha D_0^2$) plays a crucial role in all the critical parameters in Eqs. (14)-(16). This result reveals the significance of the cooperation of the ID and the two synergistic effects.

IV. CONCLUSION

In summary, we have systematically studied the behavior and mechanism of the synergistic effects of neutron and gamma ray radiation by performing successive neutron-gamma radiation experiments on input-stage PNP transistors in operational amplifier LM324N. We find that the measured input bias current obey a ‘tick’-like damage-dose curve. Two negative synergistic effects, both of which are comparable with the ID itself, have been derived from the experimental observation. The first one is caused by a carrier-induced defect annihilation in silicon; it displays as a linear function of the gamma ray dose whose slope depends quadratically on the initial DD of the samples. The second one is caused by a proton-induced defect passivation near the silica/silicon interface; it displays as an exponential function of the gamma ray dose whose amplitude shows a very strong ELDRS effect. The validity of the proposed model is also verified by the prediction of the dose for the minimal and critical synergistic damage. Our proposed mechanism demonstrates that, the ID can influence DD by decreasing the concentration of defects in it, therefore, this technique can be applied to repair devices used in the space and other extreme environments.

The authors thank Professor Chun Zheng of Institute of Nuclear Physics and Chemistry, CAEP for his kindly help in neutron radiation experiments. This work was supported by the Science Challenge Project under Grant No. TZ2016003-1 and NSFC under Grant Nos. 51672023; 11634003; U1530401.

* songyu@mtrc.ac.cn

† suhuaiwei@csrc.ac.cn

¹ H. J. Barnaby, R. D. Schrimpf, A. L. Sternberg, V. Berthe, C. R. Cirba, and R. L. Pease, IEEE Transactions on Nuclear Science **48**, 2074 (2001).

² H. J. Barnaby, S. K. Smith, R. D. Schrimpf, D. M. Fleet-

wood, and R. L. Pease, IEEE Transactions on Nuclear Science **49**, 2643 (2002).

³ J. L. Gorelick, R. Ladbury, and L. Kanchawa, IEEE transactions on nuclear science **51**, 3679 (2004).

⁴ X. Li, H. Geng, C. Liu, Z. Zhao, D. Yang, and S. He, IEEE Transactions on Nuclear Science **57**, 831 (2010).

- ⁵ X. Li, C. Liu, H. Geng, E. Rui, D. Yang, and S. He, *IEEE Transactions on Nuclear Science* **59**, 439 (2012).
- ⁶ X. Li, C. Liu, E. Rui, H. Geng, and J. Yang, *IEEE Transactions on Nuclear Science* **59**, 625 (2012).
- ⁷ X. Li, C. Liu, and J. Yang, *IEEE Transactions on Nuclear Science* **62**, 1375 (2015).
- ⁸ X. Li, C. Liu, J. Yang, and G. Ma, *IEEE Transactions on Nuclear Science* **62**, 555 (2015).
- ⁹ C. Wang, X. Bai, W. Chen, S. Yang, Y. Liu, X. Jin, and L. Ding, *Nuclear Instruments and Methods in Physics Research A* **796**, 108 (2015).
- ¹⁰ C. Wang, W. Chen, Z. Yao, X. Jin, Y. Liu, S. Yang, and Z. Wang, *Nuclear Instruments and Methods in Physics Research A* **831**, 322 (2016).
- ¹¹ X. Li, P. Li, J. Yang, and C. Liu, in *Radiation and Its Effects on Components and Systems (RADECS), 2016 16th European Conference on* (IEEE, 2016) pp. 1–4.
- ¹² X. Li, J. Yang, C. Liu, G. Bai, W. Luo, and P. Li, *Microelectronics Reliability* **82**, 130 (2018).
- ¹³ R. Pease, W. Combs, A. Johnston, T. Carriere, C. Poivey, A. Gach, and S. McClure, in *1996 IEEE Radiation Effects Data Workshop. Workshop Record. Held in conjunction with The IEEE Nuclear and Space Radiation Effects Conference* (IEEE, 1996) pp. 28–37.
- ¹⁴ H. Barnaby, R. Schrimpf, R. Pease, P. Cole, T. Turflinger, J. Krieg, J. Titus, D. Emily, M. Gehlhausen, and S. Witczak, *IEEE transactions on Nuclear Science* **46**, 1666 (1999).
- ¹⁵ J. Raymond and E. Petersen, *IEEE Transactions on Nuclear Science* **34**, 1621 (1987).
- ¹⁶ Z. Li, *IEEE Transactions on Nuclear Science* **42**, 224 (1995).
- ¹⁷ G. Lutz, *Nuclear Instruments and Methods in Physics Research Section B: Beam Interactions with Materials and Atoms* **95**, 41 (1995).
- ¹⁸ T. Schulz, H. Feick, E. Fretwurst, G. Lindstrom, M. Moll, and K. H. Mahlmann, *IEEE Transactions on Nuclear Science* **41**, 791 (1994).
- ¹⁹ Z. Li, *Nuclear Instruments and Methods in Physics Research Section A: Accelerators, Spectrometers, Detectors and Associated Equipment* **342**, 105 (1994).
- ²⁰ S. J. Watts, J. Matheson, I. H. Hopkins-Bond, A. Holmes-Siedle, A. Mohammadzadeh, and R. Pace, *IEEE Transactions on Nuclear Science* **43**, 2587 (1996).
- ²¹ G. Lindstrom, M. Ahmed, and S. e. a. Albergo, *Nuclear Instruments and Methods in Physics Research Section A: Accelerators, Spectrometers, Detectors and Associated Equipment* **466**, 308 (2001).
- ²² S. M. Myers, P. J. Cooper, and W. R. Wampler, *Journal of Applied Physics* **104**, 044507 (2008).
- ²³ R. F. Pierret and G. W. Neudeck, *Advanced semiconductor fundamentals*, Vol. 6 (Addison-Wesley Reading, MA, 1987).
- ²⁴ P. Adell and J. Boch, *Proc NSREC Short Course* (2014).
- ²⁵ R. L. Pease, R. D. Schrimpf, and D. M. Fleetwood, in *Radiation and Its Effects on Components and Systems (RADECS), 2008 European Conference on* (IEEE, 2008) pp. 18–32.
- ²⁶ N. L. Rowsey, M. E. Law, R. D. Schrimpf, D. M. Fleetwood, B. R. Tuttle, and S. T. Pantelides, *IEEE Transactions on Nuclear Science* **58**, 2937 (2011).
- ²⁷ Y. Yue, P. Li, Y. Song, and X. Zuo, *Journal of Non-Crystalline Solids* **486**, 1 (2018).
- ²⁸ S. Rashkeev, D. Fleetwood, R. Schrimpf, and S. Pantelides, *Physical review letters* **87**, 165506 (2001).
- ²⁹ D. Schmidt, A. Wu, R. Schrimpf, D. Fleetwood, and R. Pease, *IEEE Transactions on Nuclear Science* **43**, 3032 (1996).
- ³⁰ S. Kosier, A. Wei, R. Schrimpf, D. Fleetwood, M. DeLaus, R. Pease, and W. Combs, *IEEE transactions on Electron Devices* **42**, 436 (1995).
- ³¹ B. Gregory and H. Sander, *IEEE Transactions on Nuclear Science* **14**, 116 (1967).
- ³² C. Barnes, *IEEE Transactions on Nuclear Science* **16**, 28 (1969).
- ³³ J. Harrity and C. Mallon, *IEEE Transactions on Nuclear Science* **17**, 100 (1970).
- ³⁴ L. Kimerling, H. DeAngelis, and J. Diebold, *Solid State Communications* **16**, 171 (1975).
- ³⁵ L. Kimerling, *IEEE Transactions on Nuclear Science* **23**, 1497 (1976).
- ³⁶ Y. Bar-Yam and J. Joannopoulos, *Physical Review B* **30**, 1844 (1984).
- ³⁷ Y. Bar-Yam and J. Joannopoulos, *Physical Review B* **30**, 2216 (1984).
- ³⁸ R. Car, P. J. Kelly, A. Oshiyama, and S. T. Pantelides, *Physical Review Letters* **52**, 1814 (1984).
- ³⁹ S. T. Pantelides, S. N. Rashkeev, R. Buczko, D. M. Fleetwood, and R. D. Schrimpf, *IEEE Transactions on Nuclear Science* **47**, 2262 (2000).
- ⁴⁰ B. L. Sopori, X. Deng, J. P. Benner, A. Rohatgi, P. Sana, S. K. Estreicher, Y. K. Park, and M. A. Roberson, *Solar Energy Materials and Solar Cells* **41-42**, 159 (1996).
- ⁴¹ J. I. Hanoka, in *Hydrogen in Disordered and Amorphous Solids*, NATO ASI Series, Vol. 136, edited by G. Bambakidis and R. C. Bowman (Springer US, Boston, MA, 1986) pp. 81–90.
- ⁴² C. G. Van de Walle, Y. Bar-Yam, and S. T. Pantelides, *Phys. Rev. Lett.* **60**, 2761 (1988).
- ⁴³ J. W. Corbett, P. Dek, U. V. Desnica, S. J. Pearton, J. I. Pankove, and N. M. Johnson, in *Semiconductors and Semimetals*, Vol. 34 (Elsevier, 1991) pp. 49–64.
- ⁴⁴ S. C. Witczak, R. C. Laco, D. C. Mayer, D. M. Fleetwood, R. D. Schrimpf, and K. F. Galloway, *IEEE Transactions on Nuclear Science* **45**, 2339 (1998).
- ⁴⁵ S. J. Pearton, in *Thirteenth International Conf. on Defects in Semiconductors*, Metallurgical society of AIME, edited by L. C. Kimerling and J. M. Parsey (Warrendale, PA,, 1985) p. 737.
- ⁴⁶ S. B. Zhang and H. M. Branz, *Phys. Rev. Lett.* **87**, 105503 (2001).
- ⁴⁷ N. M. Johnson, *Phys. Rev. B* **31**, 5525 (1985).
- ⁴⁸ L. V. C. Assali and J. R. Leite, *Phys. Rev. Lett.* **55**, 980 (1985).
- ⁴⁹ D. Mathiot, *Phys. Rev. B* **40**, 5867 (1989).
- ⁵⁰ S. J. Pearton, J. W. Corbett, and M. Stavola, *Hydrogen in Crystalline Semiconductors*, Springer Series in Materials Science, Vol. 16 (Springer-Verlag, Berlin, 1992).
- ⁵¹ P. Sana, A. Rohatgi, J. P. Kalejs, and R. O. Bell, *Appl. Phys. Lett.* **64**, 97 (1994).
- ⁵² G. Bourret-Sicotte, P. Hamer, R. S. Bonilla, K. Collett, and P. R. Wilshaw, *Energy Procedia* **124**, 267 (2017).
- ⁵³ N. N. Gerasimenko, M. Rolle, L.-J. Cheng, Y. H. Lee, J. C. Corelli, and J. Corbett, *physica status solidi (b)* **90**, 689 (1978).